Atlantic inflow is the primary driver of remotely sensed autumn blooms in the Barents Sea.

Andrew Orkney*[1], Shubha Sathyendranath[2,3],Thomas Jackson[2],
Marie Porter[4] & Heather A. Bouman[1]

Andrew Orkney: https://orcid.org/0000-0003-4972-2541

Shubha Sathyendranath: https://orcid.org/0000-0003-3586-192X

Thomas Jackson: https://orcid.org/0000-0003-4336-1597

Marie Porter: https://orcid.org/0000-0003-3686-353X

Heather A. Bouman: https://orcid.org/0000-0002-7407-9431

1:Department of Earth Sciences, University of Oxford, OX1 3AN
2:Plymouth Marine Laboratory, PL1 3DH
3: National Centre for Earth Observation, Plymouth Marine Laboratory, PL1 3DH
4:Scottish Association for Marine Science,
Scottish Marine Institute, Oban, PA37 1QA

Running page head: Barents Sea autumn bloom dynamics
Key words: Arctic; Atlantification; Climate change; Ocean colour; Phenology; Phytoplankton

October 26, 2022

Abstract

Arctic shelf seas have historically hosted a single spring bloom, contrasting with temperate seas, where additional smaller autumn blooms occur regularly, caused by storm systems mixing nutrient rich deep waters towards the surface ocean. Post millennium, autumn blooms have increased in frequency in Arctic shelf seas. Delayed sea-ice formation, stronger autumn winds and greater inflows of nutrient rich temperate waters have all been suggested to support growing annual net primary production and an increasing incidence of autumn blooms. Here, we investigate datasets of remotely sensed September chlorophyll-a, sea surface temperature, current and wind speeds. We explore mechanistic drivers of autumn blooms in the Barents Sea, one of the most productive Arctic shelf seas, to better understand the role of strong winds and the ingression of Atlantic waters in the dynamics of autumn blooms. We perform geographically resolved regressions between remotely sensed September chlorophyll-a and environmental conditions in the Barents Sea, demonstrating a strong dependency of autumn bloom intensity on Atlantic inflow. This result highlights the importance of increased study of autumn phytoplankton bloom dynamics on Arctic shelf seas, especially the further collection and dissemination of in-situ cell count and nutrient data to determine the significance of autumn blooms for wider ecosystem function.

* Corresponding author: saxon.wessex.orkney@gmail.com

1 INTRODUCTION

The Arctic shelf seas are a productive northern ecosystem that has historically been characterised by a single intense period of phytoplankton blooms, associated with the recession and melting of sea-ice and development of a shallow, nutrient replete surface mixed-layer (Båmstedt et al. 1991, Wassmann et al. 1999). High levels of grazing by zooplankton (Cushing 1959), typically meant that Arctic autumn conditions did not favour accumulation of phytoplankton relative to losses. An increase in surface phytoplankton biomass can occur when grazing pressure from zooplankton is reduced as they begin their seasonal migration to deep waters (Longhurst 1995). However, higher phytoplankton biomass may not always result in increased primary production, because autumn sunshine may not be strong enough (Longhurst 1995, Platt et al. 2009). By comparison, a 'double-bloom' seasonal cycle occurs in the adjacent temperate North Atlantic region (González Taboada & Anadón 2014). Here, an initial spring bloom is ended by nutrient exhaustion, and a secondary autumn bloom occurs when storm systems cause the upwelling of nitrate replete deep waters (Findlay et al. 2006).

Autumn blooms have been recorded in the Barents Sea for decades, but they have been much less common than spring blooms and usually required special conditions to occur (Strass & Nöthig 1996). Indeed, the occurrence of September and October blooms in the Barents Sea has been associated with the marginal ice zone (the mosaic of sea and ice between the open ocean and pack-ice) (Hegseth 1997). These blooms may therefore have represented the final phase of the productive summer period, rather than a distinct autumn bloom akin to those in temperate seas.

Now, rapid changes to the Arctic environment are re-structuring these northern most ecosystems and their dynamics. Sea-ice extents are declining (Shapiro et al. 2003, Francis & Hunter 2007, Cavalieri & Parkinson 2012, Kwok 2018), sea surface temperatures (SST) are rising (Boitsov et al. 2012, Eriksen et al. 2017, Barton et al. 2020), and the atmosphere has become increasingly energetic (Simmonds & Keay 2009). These environmental changes may have substantial consequences for the composition of species living in Arctic communities (Lalande et al. 2013, Engel et al. 2017, Neukermans et al. 2018), the phenology (seasonal cycle of biological activity) of Arctic phytoplankton blooms (Ardyna et al. 2014, Crawford et al.

2020), their contribution of food to organisms at higher trophic levels and their role in wider biogeochemical cycles.

Increased study of Barents Sea autumn blooms and their dynamics is therefore of substantial importance. Traditionally, research effort has prioritised the spring bloom, owing to its large impact on the feeding and phenology of zooplankton communities (Søreide et al. 2010) and carbon export to the deep sea and benthos (Wassmann et al. 2006a). While the magnitude of autumn blooms is much lower than spring blooms (Dalpadado et al. 2020), the abundance, size and taxonomic composition of phytoplankton depart from non-bloom baselines (Fujiwara et al. 2018, Waga & Hirawake 2020). This means autumn blooms may play an important role in carbon export and nourishment of the planktonic food web (Tremblay et al. 2011). Indeed, autumn blooms on the Georges Bank are known to increase haddock recruitment (Leaf & Friedland 2014). Furthermore, recent research has shown an active and diverse autumn zooplanktonic community in the Barents Sea, including an annual peak in meroplankton abundance (Descôteaux et al. 2021), whose feeding could be enhanced by autumn blooms (Matsuno et al. 2015).

Environmental change has been accompanied by an increasing frequency of autumn blooms in Arctic shelf settings. Indeed, a recent review noted that autumn bloom occurrence is a 'new phenological feature' in parts of the Low Arctic (although the authors also commented that such blooms have been observed historically in Atlantic influenced regions of the Eurasian Basin) (Ardyna & Arrigo 2020). Remote sensing evidence shows that contemporary autumn blooms in the Barents Sea typically progress from north to south, reaching their greatest intensities in Atlantic influenced regions in September (Dalpadado et al. 2020, Dong et al. 2020). Barents Sea autumn blooms are dominated by non-calcifying phytoplankton (Oziel et al. 2017), distinguishing them from blooms of calcifying coccolithophores.

A variety of environmental drivers may underlie autumn bloom occurrence in the Barents Sea. It has been suggested that these blooms are initiated by declining stratification and increased upwelling of nutrient rich deep waters in September (Oziel et al. 2017). Evidence shows Arctic wind speeds have been increasing (Simmonds & Keay 2009), which may be expected to increase upwelling and trigger rapid phytoplankton growth (Morozov et al. 2015, Qu

et al. 2020). Indeed, delayed sea-ice formation and higher winds may interact over much of the Arctic shelves to facilitate autumn blooms observed at the ocean surface (Ardyna et al. 2014). However, supporting evidence for this pattern in the Barents Sea is uncertain (Ardyna et al. 2014). Some studies have suggested that high winds cause increases in remotely sensed autumn chlorophyll-a ([*chl-a*]) (Qu et al. 2020). However, other remotely sensed estimates of net primary production indicate high winds boost production in early summer (June), but not during autumn (Crawford et al. 2020).

Alternatively, inflowing Atlantic waters might facilitate local upwelling by undermining haline stratification in regions of the northern Barents Sea dominated by Arctic waters, or by shoaling above Barents Sea Water (Oziel et al. 2017). Such upwelling could support autumn blooms, especially around frontal regions (Kogeler & Rey 1999). Inflowing Atlantic waters may also deliver nutrients, that could nourish more intense blooms (Hegseth 1997, Oziel et al. 2017). Indeed, increased Atlantic influence, termed 'Atlantification', has been identified as a key force of Arctic change, viewed by many researchers as a primary driver of whole-sale ecosystem changes in the Barents Sea (Ardyna & Arrigo 2020). These changes include secular increases in remotely sensed estimates of annual net primary production (Lewis et al. 2020) and the wider dispersal and occurrence of calcifying coccolithophore blooms (Neukermans et al. 2018, Oziel et al. 2020). However, it has also been noted that a trend for declining inventories of Atlantic derived nutrients (Rey 2012, Hátún et al. 2017), might limit any role of Atlantification in the regulation of autumn bloom dynamics (Oziel et al. 2017). Increased upwelling may provide only limited nourishment to blooms if deep nutrient concentrations are insufficient to support further phytoplankton growth. Investigating the influences of Atlantic advection and local mixing events, such as storms, has therefore been identified as a key question for future research (Oziel et al. 2017). If inflowing Atlantic waters supply sufficient nutrients to support autumn blooms, a clear relationship between Atlantic inflow and remotely sensed chlorophyll-a in the surface ocean should be expected.

Rough or shallow bathymetry, which can promote water-column mixing, may also play a role modulating autumn bloom dynamics as a function of geography. Mixing over rough bathymetry helps support persistent productivity that has historically been observed around

the Spitsbergen bank and the Norwegian coast (Kogeler & Rey 1999, Not et al. 2005). Thus, a complete understanding of autumn bloom dynamics in the Barents Sea, and environmental controls on bloom intensity, has not yet fully emerged and further studies are merited.

As outlined above, previous publications have identified four possible drivers of increasing autumn bloom frequency and intensity in the Barents Sea: wind induced mixing, water-column destabilisation by Atlantic input, nutrient replenishment by Atlantic inflow and mixing over rough bathymetry (Table 1). We note that, to bring clear focus to the investigation into autumn blooms, we must take care to exclude blooms of calcifying phytoplankton, because calcifying coccolithophore blooms are a distinct phenological phenomenon from the non-calcifying autumn bloom (Oziel et al. 2017). Calcifying and non-calcifying blooms may be related to distinct environmental conditions (Neukermans et al. 2018). Pooling calcifying and non-calcifying blooms together could therefore result in a confused impression of the environmental variables that regulate autumn blooms. For example, a key hypothesis to be tested is whether energetic winds induce a deeper mixed-layer depth and thereby stimulate autumn blooms. Combining coccolithophore blooms with non-calcifying autumn blooms could obscure such a signal, if present, because the shallow mixed-layer depths that favour coccolithophores are likely to be associated with light winds.

In this paper, we employ a mask to identify and remove coccolithophore blooms in records of remotely sensed September ocean colour data in the Barents Sea. Thereafter, we produce a time-series of monthly integrations of satellite derived September chlorophyll-a ($[chl\text{-}a]$) concentrations, and explore their dependency upon SST, the frequency of energetic winds and the intensity of Atlantic inflow currents. Our study is thus designed to identify which of the potential mechanisms in Table 1 play substantial roles in the regulation of autumn bloom dynamics in the Barents Sea. We also present a version of our analysis, for which no effort has been made to mask coccolithophore blooms, (Text S1.2, Table S2, Figures S2-4).

2 MATERIALS & METHODS

2.1 Ocean Colour data

Remote sensing studies of phytoplankton concentrations are necessarily restricted to the surface ocean, where inferred [*chl-a*] is conventionally used as a proxy for phytoplankton biomass (Ardyna et al. 2014, Crawford et al. 2020, Dalpadado et al. 2020, Siswanto 2020, Silva et al. 2021). Variation in phytoplankton community composition (e.g. diatoms, nanoflagellates) can bias the inference of [*chl-a*] from ocean colour (Dutkiewicz et al. 2019), as can the development of sub-surface chlorophyll maxima, commonplace in the Eurasian Arctic in summer (Downes et al. 2020). However, previous studies have shown that surface [*chl-a*], inferred from global ocean colour products, is representative of in-situ [*chl-a*] measurements between 0-50 m depth in the Barents Sea. These results are stable across the seasonal cycle (Dalpadado et al. 2014, Dalpadado et al. 2020). Therefore, sub-surface chlorophyll maxima do not disrupt the capacity for remotely sensed [*chl-a*] to represent synoptic assessments of phytoplankton biomass at monthly temporal scales. This potential paradox could be explained by patchiness in phytoplankton blooms, which is widely reported (Wassmann et al. 2006b, Polyakova et al. 2021). Subsurface and surface [*chl-a*] is likely decoupled at a fine spatial resolution, but synonymous at larger temporal and geographic scales. Patchiness represents a major challenge in the integration of in-situ and remote sensing datasets, which are of fundamentally distinct scales. Consequently the spatial and temporal averaging of synoptic scale remote sensing data can offer insights into general ecosystem evolution that may be difficult or impossible to derive from *in-situ* observations scattered in space and time.

We therefore regard surface [*chl-a*] as a meaningful representation of phytoplankton biomass, provided it is interpreted with care. To obtain estimated of [*chl-a*], daily OC-CCIv5 (Ocean Colour Climate Change Initiative (Sathyendranath et al. 2019)) data were downloaded from the thredds server (accessed 12–27 Nov 2020)
(https://www.oceancolour.org/thredds/catalog-cci.html), for the ocean colour wavebands λ= 412, 443, 490, 510, 560 and 665 nm, at a nominal 4 km resolution, for September 2002-2019. September was chosen, because it is the month within which autumn blooms typically begin

and reach their greatest average surface [*chl-a*] in the Barents Sea (Dalpadado et al. 2020).

The OC6_MERIS ocean colour algorithm was employed to estimate [*chl-a*] concentrations from these ocean colour data (O'Reilly & Werdell 2019). Coccolithophore blooms, which tend to occur in late summer in the Barents Sea (Oziel et al. 2017) were masked, employing a modification of a previous method based on principal component decomposition (Orkney et al. 2020) (see supplement Text S1 1.1 and Figures S1-S4). It was necessary to mask coccolithophore blooms because their calcite liths scatter light, resulting in a flattened blue-to-green ratio that can manifest as apparently high [*chl-a*] in remotely sensed estimates (Supplementary Figure 1), even if the actual chlorophyll content of coccolithophore blooms is low. Previous authors have warned that coccolith production may not correlate with [*chl-a*] (Volent et al. 2011, Hovland et al. 2013, Hovland et al. 2014). We are also conscious that calcifying summer blooms, that occur between July and September, are a distinct phenological phenomenon to non-calcifying autumn blooms (Oziel et al. 2017) and therefore should not be treated as synonymous.

Following the application of a coccolithophore mask, daily [*chl-a*] estimates were averaged over each September, within 1° lat.-lon. grid cells between 0° east; 70° north; 60° east, 85° north (Figure 1) and compiled into a stack of 18 images representing maps of average [*chl-a*] for September 2002-2019. Individual observations were weighted by their surface area, a function of latitude, when computing the mean value within grid cells.

A preliminary analysis of the change in [*chl-a*] across the time-series implies that sampling biases caused by variable sea-ice and cloud cover do not significantly distort remotely sensed [*chl-a*] estimates in September (see Text S1 1.1). However, a 1 year lag between variation in wind field, inferred from scatterometer measurements, and monthly ocean colour satellite coverage, is evident over the time-series. An inter-annual persistence in the relationship between open water area and wind field could be consistent with the 'wind feedback' loop identified by Smedsrud et al. (2013). However, it should be noted that observational records are not long enough to confirm the operation of the wind feedback loop in the Barents Sea (Smedsrud et al. 2013). Inter-annual persistence means that time-series of environmental variables in the Barents Sea are likely to exhibit temporal autocorrelation (Dalpadado et al. 2014). Analyses must therefore be designed to accommodate temporal autocorrelation, which can cause type-1

statistical errors when assessing the significance of regressions (Santer et al. 2008) (see Section 2.3). This is because the n sets of measurements in a time-series are not truly statistically independent when temporal autocorrelation is present, a key assumption that underlies many conventional statistical methods.

2.2 Environmental data

We sought monthly environmental data for hydrographic variables from the ARCTIC_REANALYSIS_PHYS_002_003 dataset, which we obtained from CMEMS (Copernicus Marine Environment Monitoring Service: https://marine.copernicus.eu/). (Physical reanalysis product for hydrographic conditions) Direct dataset link: `https://resources.marine.copernicus.eu/product-detail/ARCTIC_REANALYSIS_PHYS_002_003/INFORMATION` (accessed 01–06 Dec 2020).

ARCTIC_REANALYSIS_PHYS_002_003 is a reanalysis product offering SST, salinity and current speed data, derived from assimilated sea level altimetry. The product is produced by a coupled ocean and sea-ice data assimilation (TOPAZ4) and the HYCOM ocean model, which performs well reproducing surface measurements (Xie et al. 2017).

The September SST and salinity data were averaged within 1° lat.-lon. grid cells between 0° east; 70° north; 60° east, 85° north, in order to create a stack of 18 average monthly images of September conditions over the Barents Sea.

In-situ observations in the Norwegian Sea show that silicic acid is abundant in biologically relevant concentrations across the seasonal cycle (Findlay et al. 2008). The advection of surface Atlantic Waters from the Norwegian Sea is therefore likely to redistribute nutrient inventories. We employ a similar approach to Oziel et al. (2020) to contrive a measure of surface Atlantic inflow. Oziel et al. computed geostrophic surface velocities, which are known to reflect underlying patterns of ocean circulation (Raj et al. 2018), from remotely-sensed sea level altimetry data. We computed monthly average September current speed from the Euclidean distance defined by the meridional and zonal components for each data point in the altimetry-derived current speed dataset. The magnitudes were then averaged within each grid cell. Thereafter,

we computed a time-series of average current speed between 70-75° north 0-20° east to represent the strength of prevailing surface Atlantic inflow from the Norwegian Sea. Daily September wind speed data was also sought from CMEMS, from the WIND_GLO_WIND_L3_REP_OBSERVATIONS_012_005 gridded scatterometer derived wind speed measurements. Direct dataset link: `https://resources.marine.copernicus.eu/product-detail/WIND_GLO_WIND_L3_REP_OBSERVATIONS_012_005/INFORMATION` (accessed 02 Dec 2020). Data at a 25 km resolution from ascending passes of the SeaWinds instrument aboard the QuikScat satellite were downloaded for the interval September 2002-2009, while data at a 25 km resolution from ascending passes of the ASCAT instrument of the MetOp-A satellite were downloaded for the interval September 2010-2019. The number of days experiencing wind speeds above 10 ms^{-1} (similar to a previous metric for energetic wind events (Ardyna et al. 2014)) was then computed for each unique location. The mean number of such windy days in each September was computed within each grid cell. Observations were weighted in accordance with their latitude (as the projection was not stereographic). A complete stack of 18 images of gridded SST, salinity, current and wind speed data was thus assembled, representing the inter-annual evolution of September environmental conditions.

2.3 Analysis

We accommodated the possibility of a 1 year temporal autocorrelation in our study (see dataset and methods) by designing an analytical frame-work that explicitly tests for temporal autocorrelation. We performed Generalised Least Squares (GLS) regressions with the gls function of the nlme R package, version 3.1-144 (Pinheiro et al. 2020), both with and without 1 year autocorrelation represented. Autocorrelated fits were implemented with the corAR1 function of the R nlme package. The R stats analysis of variance (anova) function was then used to compare fits and the autocorrelated model was selected if it was significantly favoured at a 0.05 alpha level. GLS is a method for estimation of model fit parameters in regressions. GLS differs from Ordinary Least Squares approaches (that minimise Euclidean distance between the fitted and observed values) by accounting for the underlying variance structure in model

residuals. Structure in the variety of residuals (difference between fitted and observed values) is common place in time-series data, as a result of statistical non-independence between observations. Periodicity or greater similarity between observations that are separated by less time may cause this structure, which is known as autocorrelation. In GLS, the covariance matrix of the residuals is employed in the estimation of the fit parameters. GLS approaches can therefore provide more robust model fits to data where underlying variance structures exist, such as in time-series.

Our initial analysis simply computed the linear trends in the variation of [*chl-a*], SST, windy days and current speed within grid cells (Figure 2), in order to reveal how conditions have changed over time. We then computed the linear relationships between gridded [*chl-a*] and SST, windy days and current speed, in order to test whether the environmental variables individually explain variation in autumn bloom intensity (Figure 3). Figure 2 therefore represents secular trends, while Figure 3 provides insight into their possible mechanistic relationships. We also computed the relationship between gridded SST and windy days, as we expected that vertical overturning of the ocean, engendered by windy events, should alter SST. This therefore represents a test of the realism of the interaction of the reanalysis products we employed to represent environmental variability.

We investigated the relationships between [*chl-a*] and the current speed in the inflow region of the Barents Sea, which we defined as being south of 75° north and west of 20° east- see Figure 1, between the inter-annual differences of these two variables; and between the inter-annual differences of [*chl-a*] and the frequency of windy days (Figure 4). In these final analyses we projected maps of confidence intervals of the geographic occurrence of Atlantic derived water masses (defined as having SST >3°C and salinity >34.8‰ (Oziel et al. 2016, Våge et al. 2016)). We have also plotted the variance normalised shelf-wide trends in [*chl-a*] and the environmental variables, weighted by surface area, so that the variation in the time-series at a synoptic scale may be inspected visually (Figure 4d). Generalised Least Squares models for pairwise combinations of shelf-wide relationships are presented in Table 2, Figure S5 and discussed further in Text S1.3. Model fits are compared by computing the Akaike Information Criterion (AIC) with a correction for small sample sizes (AICc).

AIC summarises information lost representing observations by a model fit. Additional model parameters might minimise model residuals, even if there are no underlying relationships; a situation known as 'over-fitting'. AIC is therefore designed to penalise additional model parameters. AIC values therefore indicate a balance between information loss and model complexity, and typically the model with the smallest AIC is preferred. AIC scores can only compare models describing the same dataset of dependent variables. When sample sizes are small, AIC tends to select over-fit models with a large number of parameters. Therefore, for small sample sizes, a bespoke additional term can be added that adjusts the penalty on the number of model parameters as a function of sample size. This produces the 'AICc' score, which can be treated similarly to AIC as an index of model performance. We employ the AICcmodavg R package to calculate AICc (Mazerolle 2020).

All analyses were undertaken in R version 3.6.3.

Re-gridded data used in our analyses, and illustrative codes that can be applied to reproduce the figures herein, are available in the following Github repository:

https://github.com/aorkney/Autumn

Zenodo url: https://zenodo.org/record/5525075#.YUyyNH3TWGY

DOI: 10.5281/zenodo.5525075

Data citation: aorkney. (2021). aorkney/Autumn: Autumn bloom code release (v1.0). Zenodo. https://doi.org/10.5281/zenodo.5525075

3 RESULTS

We found strong evidence of increasing autumn bloom intensity in the Barents Sea (Figure 2a), with increases most pronounced near the Atlantic inflow region (Figure 1). SST increases were consistent with previous reports in the literature (Figure 2b) (Barton et al. 2020). Changes in the frequency of windy days were uncertain, with the exception of increases in the far north-east (Figure 2c). Current speeds showed evidence of increasing inflow onto the shelf (Figure 2d) but declining speeds in the Fram Strait. This secular trend directly reflects the increase in

surface current velocities reported by Oziel et al. (Oziel et al. 2020) (see Figure 3c), which the authors found to play a key role in the increasing dispersal of temperate phytoplankton into Arctic settings. We suggest this pattern of wind and current changes is consistent with the expectation that winds in the northern Barents Sea regulate the routes that Atlantic waters take as they flow into the Arctic region (Lien et al. 2013).

We found that SST is well correlated with autumn bloom intensity, especially close to the inflow region (Figure 3a). This observation is compatible with reports of more intense autumn blooms in years with lower sea-ice extents (Oziel et al. 2017). The relationship between autumn bloom intensity and windy days simply reproduces multi-annual trends in windy days (Figure 3b). This may suggest that, rather than autumn bloom intensity depending substantially on windiness, both variables simply have a common dependency on time. We note that a previous study did not observe a strong relationship between wind and autumn blooms in the Barents Sea (Ardyna et al. 2014). However, the time period examined (1998-2012) precedes the period of most sustained autumn [*chl-a*] increases (Figure 4d) in this study. Geographically resolved (local) current speed shows some significant positive associations with autumn bloom intensity in the inflow region (Figure 3c). An assessment of wind and SST shows the anticipated physical relationships. It is likely that windy days mix warmer waters to the surface in the far northern haline-stratified sea, while they mix cooler deep waters towards the surface in more southern temperature-stratified seas (Figure 3d) (Carmack 2007).

Inflow current speed (defined as the current speed in the inflow region of Figure 1, that is outlined with a cyan box) and autumn bloom intensity show a strong positive relationship (Figure 4a), as do their inter-annual differences (Figure 4b). The strongest signal is evident in the Atlantic inflow region south-west of Bjørnøya. The inter-annual differences of autumn bloom intensity and wind show a slightly negative relationship in the inflow region (Figure 4c), indicating that windier years are associated with depressed bloom intensity in this region. This is a surprising finding, given that Figure 3d demonstrates that winds are likely to cause vertical mixing, which is reported in the literature to play a key role in autumn bloom onset (Oziel et al. 2017, Qu et al. 2020). However, these findings do not necessarily contradict one another; mechanisms regulating bloom onset and bloom intensity may be distinct. The secular variance

normalised trends in bloom intensity, SST, inflow current speed and windiness are displayed in Figure 4d, where it is clear inflow current speed possesses the strongest relationship to bloom intensity. These results are reinforced by our Generalised Least Squares models (Table 2). We note that inter-annual differences in [*chl-a*] and average inflow current speed only begin to follow each other closely after 2009. We note that inter-annual variation in SST is often not clearly related to inter-annual variation in either surface inflow current speed or [*chl-a*]. SST is modulated by windiness, which could undermine its correlation with other variables. Attempts to qualify the role that shallow bathymetry might play supporting inter-annual increases in [*chl-a*], or its relationship to inflowing current speed, are presented in Text S1 1.3 and Figure S6. The sense of any relationship is unclear.

4 DISCUSSION

Our leading finding is a strong relationship between autumn bloom [*chl-a*] and the speed of currents in the Atlantic inflow region (Figure 4 and Table 2). We do not find a clear relationship between autumn bloom [*chl-a*] and windy days, except in the far north-east, close to the interior Eurasian shelf seas (Figure 3b and 4c). Curiously, in some sectors of our study area, high winds significantly depress [*chl-a*] (Figure 4c). Unlike other Arctic shelf seas, increases in autumn [*chl-a*] in the Barents Sea cannot be attributed to a longer growing season or alleviation of light limitation (resulting for example from reduced sea-ice extents) because the southern Barents Sea is perennially ice free (Shapiro et al. 2003).

We found a strong positive dependency of autumn bloom intensity upon SST (Figure 3a). This accords with a previous report of more intense autumn blooms in years with lower sea-ice extents (Oziel et al. 2017). This finding may at first appear counter-intuitive, given that, within individual years, autumn bloom onset is generally accompanied by a decline in SST as deeper waters are mixed to the surface (Oziel et al. 2017, Qu et al. 2020). We hypothesise that the inter-annual relationship between autumn bloom intensity and SST results from SST acting as a tracer of Atlantic Water delivery, rather than because a multi-annual trend towards

higher SST plays any direct role in stimulating blooms. Alternatively, it is possible that cooler years, with greater sea-ice extent, are accompanied by greater haline stratification, impeding autumnal upwelling and therefore depressing bloom intensity (Oziel et al. 2017). Investigating the exact mechanism underlying the relationship between [*chl-a*] and SST is a subject of future study, that will require in-situ biological and hydrographic samples.

Inflowing Atlantic waters might initiate blooms either by destabilising haline stratification (in the northern Barents Sea), shoaling over denser Barents Sea Water (in frontal regions), or by replenishing nutrient inventories. It is possible that water-column destabilisation might interact with variation in windiness to stimulate autumn blooms, but we do not find clear evidence of this here. The geographic distribution of relationships we uncover is most consistent with a hypothesis of Atlantic ingression replenishing diminished nutrient supplies. The strongest increase in [*chl-a*] is in the Atlantic inflow region, (Figure 2a) as are the strongest dependencies of [*chl-a*] on SST (Figure 3a) and Atlantic inflow (Figure 4a-b).

A working hypothesis, that Atlantic recharge of deep nutrient inventories plays a first-order role in the regulation of autumn blooms in the Barents Sea, is consistent with a recent study of oxygen and nitrogen isotopes (Tuerena et al. 2021). Measurements of δ^{15}N-NO_3 imply that Barents Sea production depends on Atlantic inflow nitrate, while δ^{18}O-NO_3 values in Arctic waters indicate long-term integration of Atlantic derived nitrate (Tuerena et al. 2021). This could explain the weaker relationship in Arctic waters between inter-annual variation in autumn bloom intensity and average current speed in the inflow region (see Figure 4a-b).

While bathymetry guides the inflow of Atlantic waters onto the shelf (Oziel et al. 2016) (see Figure 4, where Atlantic ingression is confined by the Spitsbergen bank south of Svalbard), and is therefore inseparable from its role in autumn bloom onset, we do not find any evidence that shallow bathymetry enhances inter-annual trends towards higher [*chl-a*], or that it modulates other environmental drivers (see Text S1 1.3 and Figure S6). This suite of findings helps constrain our understanding of the environmental drivers of Autumn blooms in the Barents Sea (Table 3).

However, open questions remain; such as how these observations can be reconciled with previous literature attesting to a positive association between wind speed and autumn [*chl-a*]

(Qu et al. 2020). In addition, the inter-annual differences between high wind events and autumn [*chl-a*] anticorrelate in the Atlantic inflow region (Figure 4c). The theoretical equations of Findlay et al. (2006) may offer a route to combine our findings into a coherent synthesis. Autumn blooms are inherently disequilibrium processes, the evolution of which is initiated by a rapid increase in mixed-layer depth and controlled by the initial conditions established by the previous history of the water-column (Findlay et al. 2006). The difference between surface and deep nutrient concentration, grazer populations that may affect phytoplankton losses, and the initial phytoplankton population size all influence the evolution of quasi-stable autumn blooms (Findlay et al. 2006). Rapid deepening of the mixed-layer may import nutrients into the sunlit surface ocean, and may disperse grazer populations, both of which may allow phytoplankton growth rates to temporarily exceed losses and hence cause a bloom. However, should the same physical conditions develop very gradually, then the delivery of deep nutrient stores will occur at a more modest rate and phytoplankton losses, which export nutrients to the deep ocean, may keep pace with growth. Hence, the initiation and evolution of an autumn bloom depends on dynamic changes in vertical mixing, combined with complex dependencies on the initial system state.

Thus, in the salinity-stratified north-eastern waters of the Barents Sea, and the interior Eurasian shelves, we suggest that windy days represent significant excursions from equilibrium. Rapid mixed-layer deepening therefore mixes a rich supply of deep nutrients towards the surface ocean and triggers intense blooms; as suggested by Ardyna et al. (2014). By contrast, in the south-western Barents Sea, windy days are a routine occurrence. Episodic upwelling over the productive season means deeper nutrient stocks have been more depleted before the autumn by summer blooms (Morozov et al. 2015). The difference between surface and deeper nutrient concentrations may therefore be smaller, and rapid mixed-layer deepening in the autumn may not import sufficient new nutrients to cause a substantial increase in surface nutrient concentrations. This is consistent with recent findings that high winds cause greater primary production in the Barents Sea during the summer (Crawford et al. 2020). In addition to vertical mixing, horizontal advection of Atlantic inflow during or before the autumn is likely to re-stock nutrient inventories. This hypothesis provides an explanation for the

clear relationship uncovered here between the September inflow current speed, a key source of essential nutrients, and the concentration of autumn [*chl-a*] inferred by analysis of remotely sensed ocean colour. This hypothesis also explains the relationship between autumn [*chl-a*] and SST, especially in the south-west (Figure 3a), because SST acts as a tracer of the delivery of warm Atlantic derived waters to the shelf. A dependency of September [*chl-a*] on SST (Table 2) probably reflects variation in the delivery of Atlantic Water, or may reflect an inter-annual trend towards higher Atlantic Water temperatures (Boitsov et al. 2012).

We also note that local vertical mixing may inhibit blooms if it is too intense, by mixing phytoplankton cells deeper into the water-column (Oziel et al. 2017). This would have the effect of temporarily decreasing [*chl-a*] detected at the surface ocean (Morozov et al. 2015) and would ultimately cause light limitation, depressing phytoplankton growth. This could explain why there is a negative correlation between the inter-annual differences in windy days and autumn [*chl-a*] (Figure 4c; Table 2- dependency of biomass on wind). Supporting this perspective, the single region in the Atlantic inflow that does not exhibit a significant relationship between [*chl-a*] and inflow current speed (just south-west of the Svalbard Archipelago) is typified by a slight increase in high winds (Figure 2c). In addition, inter-annual differences of [*chl-a*] and storminess anti-correlate significantly here (Figure 4c). Strong winds south-west of Svalbard may therefore undermine autumn blooms, even in circumstances when Atlantic Water delivery has re-stocked nutrient inventories.

Alternatively, variation in windy day frequency often lags variance in SST by a year (see Figure 4d). Thus, years with high Atlantic Water delivery, intense autumn blooms and high SST, are often followed by years with a high frequency of windy days. Years with unusually intense autumn blooms are usually followed by a decline in bloom intensity, as a consequence of regression to the mean. It is therefore possible that an illusion of a negative relationship between variance in windy day frequency and autumn [*chl-a*] may be established. In support of this hypothesis, we note that a GLS model of the dependency of windy days upon SST exhibits significant temporal autocorrelation, a significant p-value (0.017) and an overall negative relationship (Table 2- dependency of wind on SST). AICc values in Table 2 indicate that this relationship is the most supported interaction between any two environmental variables in our

study.

A key ambition of future research, necessary to place our findings in context, should be the systematic description of the phytoplankton community composition of autumn blooms in the Barents Sea. To date, publications have described modest chlorophyll-a concentrations $\approx 2.2\,\mathrm{mg\,m^{-3}}$ along the marginal ice zone, dominated by sympagic and boreal diatom genera (Chaetoceros, Leptocylindrus, Nitzschia, Thalassiosira) (Hegseth 1997, Heimdal 1983). Sampling in the White and Laptev Seas has tended to indicate low accumulations of heterotrophic dinoflagellate biomass, with occasional diatom blooms when nutrient invetories permit (Ilyash et al. 2011, Polyakova et al. 2021). None of these works have, however, focused primarily on the perenially ice-free open ocean of the south-west Barents Sea, where autumn blooms are most intense. The collection and dissemination of microscopic descriptions, hydrography and nutrient assays is therefore advocated.

4.1 Limitations

The dilution of intense sub-surface blooms (Downes et al. 2020) by high winds may increase surface $[chl\text{-}a]$, providing an illusory impression that biomass has increased. However, the widespread validation of surface and *in-situ* $[chl\text{-}a]$ and remote-sensing inferences indicates this bias does not affect monthly remote-sensing integrations produced over large geographic scales.

Krill populations, which may graze phytoplankton blooms, may be imported to the Barents Sea by inflow events (Eriksen et al. 2017). Grazers might depress autumn blooms. Moreover, zooplankton may themselves bias inference of $[chl\text{-}a]$ from remotely sensed ocean colour high, because the rich pigmentation in their bodies can be mistaken for chlorophyll-a (Basedow et al. 2019). Autumn delivery of zooplankton to the north Norwegian coast by Atlantic inflow currents has recently been reported (Coguiec et al. 2021). We consider investigation of these potential biases beyond the scope of our current research. As yet, no remote sensing algorithm has been developed to distinguish swarms of zooplankton. Modelling of autumn bloom dynamics incorporates, and is sensitive to, variation in the initial value of a phytoplankton mortality term. This mortality term implicitly includes the effects of grazing (Findlay et al.

2006). Thus, an empirical exploration of the role of grazers should be a major ambition of future research to address remaining knowledge gaps.

We note that inventories of essential macronutrients in the Barents Sea, such as nitrate (Oziel et al. 2017), and silicic acid (Rey 2012), have been declining over an inter-annual time scale, and that these declines have been attributed to upstream processes outside of the Barents Sea (Hátún et al. 2017). This may represent a potential challenge to suggestions that increasing Atlantic inflow currents provide enhanced nutrient supply to autumn blooms. In-situ observations indicate silicic acid is never depleted in the surface Norwegian Sea (Findlay et al. 2008), suggesting that a secular decline in Atlantic Water nutrient concentrations is unlikely to limit autumn phytoplankton blooms, at least in the immediate future. The ongoing investigation of declining nutrient inventories, and their effects on Barents Sea phytoplankton phenology, merits further research.

Our remote sensing approach and use of a global algorithm agnostic to local phytoplankton bio-optical variation may mean that some variation in perceived biomass is driven by variability in phytoplankton community composition (Dutkiewicz et al. 2019), for example as a result of changing dispersal patterns and source populations (Oziel et al. 2020). We have attempted to isolate and remove such a signal, by masking optically and phenologically distinct (Oziel et al. 2017) coccolithophore blooms from non-calcifying autumn phytoplankton. It is also possible that variation in cloud and ice fields influences the likelihood of perceiving blooms (Jönsson et al. 2020). We, furthermore, are unable to investigate ice-affiliated modes of production, or sub-surface blooms, which develop over summer (Downes et al. 2020) and may be re-invigorated by upwelling of deep nutrients in autumn.

The further testing of the hypotheses we have generated here will require the analysis of in-situ $[chl\text{-}a]$ measurements, nitrate and silicic acid concentrations above and below the mixed layer, with current data. The integration of these data with phytoplankton community compositional data, such as cell counts, would provide further insight into the significance of Barents Sea autumn blooms.

4.2 Conclusion

Vertical mixing of the ocean is known to initiate autumn blooms in the Barents Sea by breaking down water-column stratification and allowing nutrient depleted surface waters to be recharged with deep sourced nutrients. Our analysis shows energetic winds promote mixing, however inter-annual variance in the frequency of windy days does not explain variation in autumn bloom biomass, detected by remotely sensed ocean colour. Instead, this variation is explained well by variance in average surface current speed of Atlantic waters in the south-western Barents Sea during September. We suggest a similar relationship between bloom biomass and sea surface temperature exists because temperature is a surrogate for Atlantic water contribution. Atlantic water is rich in nutrients essential to support phytoplankton growth, and therefore autumn blooms in the Barents Sea may depend on the quantity of new Atlantic water delivered to the surface ocean during or just before autumn. Windy days are relatively common in the Barents Sea, compared with other parts of the Arctic, therefore variance in their frequency may not critically limit the vertical supply of nutrients at a local scale. We suggest an inter-annual trend for greater Atlantic inflow in the surface ocean (Atlantification) supports increasing autumn bloom biomasses in the Barents Sea. However, Atlantic nutrient inventories have been in decline in recent years, prompting us to question how multiple controls on nutrient provision will influence the phenology of autumn blooms in the future in the Barents Sea.

5 ACKNOWLEDGEMENTS

We acknowledge research funding from the Natural Environment Research Council (NERC)
Grant number: NE/P006507/1 (Heather Bouman and Andrew Orkney)
Grant number: NE/P006302/1 (Marie Porter)
This work is a contribution to the Simons Foundation Project Computational Biogeochemical Modeling of Marine Ecosystems (CBIOMES, number 549947, S.S.). This paper is a also a contribution to the ESA projects Ocean Colour Climate Change Initiative (OC-CCI); and Biological Pump and Carbon Exchange Processes (BICEP). Additional support from the National Centre for Earth Observation (UK) is also gratefully acknowledged.

Environmental datasets were obtained from CMEMS (Copernicus Marine environment monitoring service: https://marine.copernicus.eu/), and hence we acknowledge the service and its European Union funding.

Raphaëlle Descôteaux provided expert input on zooplankton phenology and dynamics in the Barents Sea, and the significance this may confer for autumn phytoplankton blooms to wider ecosystem function.

6 LITERATURE CITED

Ardyna M, Arrigo KR (2020) Phytoplankton dynamics in a changing Arctic Ocean. Nat Clim Change 10(10):892–903

Ardyna M, Babin M, Gosselin M, Devred E, Rainville L, Tremblay JÉ (2014) Recent Arctic Ocean sea ice loss triggers novel fall phytoplankton blooms. Geophys Res Lett 41(17):6207–6212

Båmstedt U, Eilertsen HC, Tande KS, Slagstad D, Skjoldal HR (1991) Copepod grazing and its potential impact on the phytoplankton development in the Barents Sea. Polar Res 10(2):339–354

Barton BI, Lenn YD, Lique C (2020) Observed atlantification of the Barents Sea causes the polar front to limit the expansion of winter sea ice. J Phys Oceanogr 500:18–0003

Basedow SL, McKee D, Lefering I, Gislason A, Daase M, Trudnowska E, Egeland ES, Choquet M, Falk-Petersen S (2019) Remote sensing of zooplankton swarms. Sci Rep 9(1):686

Boitsov VD, Karsakov AL, Trofimov AG (2012) Atlantic water temperature and climate in the Barents Sea, 2000–2009. ICES J Mar Sci 69(5):833–840

Carmack E (2007) The alpha/beta ocean distinction: A perspective on freshwater fluxes, convection, nutrients and productivity in high-latitude seas. Deep Sea Res II 54(23-26):2578–2598

Cavalieri DJ, Parkinson CL (2012) Arctic sea ice variability and trends, 1979-2010. The Cryosphere 6(4):881

Coguiec E, Ershova EA, Daase M, Vonnahme TR, Wangensteen OS, Gradinger R, Præbel K, Berge J (2021) Seasonal variability in the zooplankton community structure in a sub-arctic fjord as revealed by morphological and molecular approaches. Front Mar Sci 8:1049

Crawford AD, Krumhardt KM, Lovenduski NS, van Dijken GL, Arrigo KR (2020) Summer high-wind events and phytoplankton productivity in the Arctic Ocean. J Geophys Res, C, Oceans 125(9):e2020JC016565

Cushing D (1959) The seasonal variation in oceanic production as a problem in population dynamics. ICES J Mar Sci 24(3):455–464

Dalpadado P, Arrigo KR, Hjøllo SS, Rey F, Ingvaldsen RB, Sperfeld E, Van Dijken GL, Stige LC, Olsen A, Ottersen G (2014) Productivity in the Barents Sea-response to recent climate variability. PLOS ONE 9(5):e95273

Dalpadado P, Arrigo KR, van Dijken GL, Skjoldal HR, Bagøien E, Dolgov AV, Prokopchuk IP, Sperfeld E (2020) Climate effects on temporal and spatial dynamics of phytoplankton and zooplankton in the Barents Sea. Prog Oceanogr 185:102320

Descôteaux R, Ershova E, Wangensteen OS, Præbel K, Renaud PE, Cottier F, Bluhm BA (2021) Meroplankton diversity, seasonality and life-history traits across the Barents Sea polar front revealed by high-throughput DNA barcoding. Front Mar Sci 8:609

Dong K, Kvile KØ, Stenseth NC, Stige LC (2020) Associations among temperature, sea ice and phytoplankton bloom dynamics in the Barents Sea. Mar Ecol Prog Ser 635:25–36

Downes PP, Goult SJ, Woodward EMS, Widdicombe CE, Tait K, Dixon JL (2020) Phosphorus dynamics in the Barents Sea. Limnol Oceanogr 66:S326–S342

Dutkiewicz S, Hickman AE, Jahn O, Henson S, Beaulieu C, Monier E (2019) Ocean colour signature of climate change. Nat Commun 10(1):578

Engel A, Piontek J, Metfies K, Endres S, Sprong P, Peeken I, Gäbler-Schwarz S, Nöthig EM (2017) Inter-annual variability of transparent exopolymer particles in the Arctic Ocean reveals high sensitivity to ecosystem changes. Sci Rep 7(1):4129

Eriksen E, Skjoldal HR, Gjøsæter H, Primicerio R (2017) Spatial and temporal changes in the Barents Sea pelagic compartment during the recent warming. Prog Oceanogr 151:206–226

Findlay H, Tyrrell T, Bellerby R, Merico A, Skjelvan I (2008) Carbon and nutrient mixed layer dynamics in the Norwegian Sea. Biogeosciences 5(5):1395–1410

Findlay HS, Yool A, Nodale M, Pitchford JW (2006) Modelling of autumn plankton bloom dynamics. J Plankton Res 28(2):209–220

Francis JA, Hunter E (2007) Drivers of declining sea ice in the Arctic winter: A tale of two seas. Geophys Res Lett 34(17)

Fujiwara A, Nishino S, Matsuno K, Onodera J, Kawaguchi Y, Hirawake T, Suzuki K, Inoue J, Kikuchi T (2018) Changes in phytoplankton community structure during wind-induced fall bloom on the central Chukchi Shelf. Polar Biol 41(6):1279–1295

González Taboada F, Anadón R (2014) Seasonality of North Atlantic phytoplankton from space: impact of environmental forcing on a changing phenology (1998–2012). Glob Change Biol 20(3):698–712

Hátún H, Azetsu-Scott K, Somavilla R, Rey F, Johnson C, Mathis M, Mikolajewicz U, Coupel P, Tremblay JÉ, Hartman S, et al. (2017) The subpolar gyre regulates silicate concentrations in the North Atlantic. Sci Rep 7(1):1–9

Hegseth EN (1997) Phytoplankton of the Barents Sea- the end of a growth season. Polar Biol 17(3):235–241

Heimdal BR (1983) Phytoplankton and nutrients in the waters north-west of Spitsbergen in the autumn of 1979. J Plankton Res 5(6):901–918

Hovland EK, Dierssen HM, Ferreira AS, Johnsen G (2013) Dynamics regulating major trends in Barents Sea temperatures and subsequent effect on remotely sensed particulate inorganic carbon. Mar Ecol Prog Ser 484:17–32

Hovland EK, Hancke K, Alver MO, Drinkwater K, Høkedal J, Johnsen G, Moline M, Sakshaug E (2014) Optical impact of an *Emiliania huxleyi* bloom in the frontal region of the Barents Sea. J Mar Syst 130:228–240

Ilyash L, Radchenko I, Shevchenko V, Lisitzin A, Paka V, Burenkov V, Novigatskiy A, Chul'tsova A, Pantyulin A (2011) Spatial distribution of phytoplankton in the White Sea in the late summer period with regard to the water structure and dynamics. Oceanology 51(6):993–1003

Jönsson BF, Sathyendranath S, Platt T (2020) Trends in winter light environment over the Arctic Ocean: A perspective from two decades of ocean color data. Geophys Res Lett 47(16):e2020GL089037

Kogeler J, Rey F (1999) Ocean colour and the spatial and seasonal distribution of phytoplankton in the Barents Sea. Int J Remote Sens 20(7):1303–1318

Kwok R (2018) Arctic sea ice thickness, volume, and multiyear ice coverage: losses and coupled variability (1958–2018). Environ Res Lett 13(10):105005

Lalande C, Bauerfeind E, Nöthig EM, Beszczynska-Möller A (2013) Impact of a warm anomaly on export fluxes of biogenic matter in the eastern Fram Strait. Prog Oceanogr 109:70–77

Leaf RT, Friedland KD (2014) Autumn bloom phenology and magnitude influence haddock recruitment on Georges Bank. ICES J Mar Sci 71(8):2017–2025

Lewis K, Van Dijken G, Arrigo KR (2020) Changes in phytoplankton concentration now drive increased Arctic Ocean primary production. Science 369(6500):198–202

Lien VS, Vikebø FB, Skagseth Ø (2013) One mechanism contributing to co-variability of the Atlantic inflow branches to the Arctic. Nat Commun 4(1):1–6

Longhurst A (1995) Seasonal cycles of pelagic production and consumption. Prog Oceanogr 36(2):77–167

Matsuno K, Yamaguchi A, Nishino S, Inoue J, Kikuchi T (2015) Short-term changes in the mesozooplankton community and copepod gut pigment in the Chukchi Sea in autumn: reflections of a strong wind event. Biogeosciences 12(13):4005–4015

Mazerolle MJ (2020) Aiccmodavg: Model selection and multimodel inference based on (q)aic(c). https://cranr-projectorg/package=AICcmodavg R package version 2.3-1

Morozov E, Kondrik D, Fedorova A, Pozdnyakov D, Tang D, Pettersson L (2015) A spaceborne assessment of cyclone impacts on Barents Sea surface temperature and chlorophyll. Int J Remote Sens 36(7):1921–1941

Neukermans G, Oziel L, Babin M (2018) Increased intrusion of warming Atlantic water leads to rapid expansion of temperate phytoplankton in the Arctic. Glob Change Biol 24(6):2545–2553

Not F, Massana R, Latasa M, Marie D, Colson C, Eikrem W, Pedrós-Alió C, Vaulot D, Simon N (2005) Late summer community composition and abundance of photosynthetic picoeukaryotes in Norwegian and Barents Seas. Limnol Oceanogr 50(5):1677–1686

O'Reilly JE, Werdell PJ (2019) Chlorophyll algorithms for ocean color sensors-OC4, OC5 and OC6. Remote Sens Environ 229:32–47

Orkney A, Platt T, Narayanaswamy BE, Kostakis I, Bouman HA (2020) Bio-optical evidence for increasing *Phaeocystis* dominance in the Barents Sea. Philos Trans R Soc Lond, A 378(2181):20190357

Oziel L, Baudena A, Ardyna M, Massicotte P, Randelhoff A, Sallée JB, Ingvaldsen RB, Devred E, Babin M (2020) Faster Atlantic currents drive poleward expansion of temperate phytoplankton in the Arctic Ocean. Nat Commun 11(1):1–8

Oziel L, Neukermans G, Ardyna M, Lancelot C, Tison JL, Wassmann P, Sirven J, Ruiz-Pino D, Gascard JC (2017) Role for Atlantic inflows and sea ice loss on shifting phytoplankton blooms in the Barents Sea. J Geophys Res, C, Oceans 122(6):5121–5139

Oziel L, Sirven J, Gascard JC (2016) The Barents Sea frontal zones and water masses variability (1980–2011). Ocean Sci 12(1):169–184

Pante E, Simon-Bouhet B (2013) marmap: A package for importing, plotting and analyzing bathymetric and topographic data in R. PLOS ONE 8(9):e73051

Pinheiro J, Bates D, DebRoy S, Sarkar D, R Core Team (2020) nlme: Linear and nonlinear mixed effects models. https://CRANR-projectorg/package=nlme R package version 3.1-144

Platt T, White III GN, Zhai L, Sathyendranath S, Roy S (2009) The phenology of phytoplankton blooms: Ecosystem indicators from remote sensing. Ecol Modell 220(21):3057–3069

Polyakova YI, Kryukova I, Martynov F, Novikhin A, Abramova E, Kassens H, Hölemann J (2021) Community structure and spatial distribution of phytoplankton in relation to hydrography in the Laptev Sea and the East Siberian Sea (autumn 2008). Polar Biol 44(7):1229–1250

Qu B, Gabric AJ, Zeng M, Liu X (2020) Correlations among phytoplankton biomass, sea ice and wind speed in Barents Sea and the future climate trends. Polar Sci 24:100525

Raj RP, Nilsen JØ, Johannessen J, Furevik T, Andersen O, Bertino L (2018) Quantifying Atlantic Water transport to the Nordic Seas by remote sensing. Remote Sens Environ 216:758–769

673 Rey F (2012) Declining silicate concentrations in the Norwegian and Barents Seas. ICES J
674 Mar Sci 69(2):208–212

675 Santer BD, Thorne P, Haimberger L, Taylor KE, Wigley T, Lanzante J, Solomon S, Free M,
676 Gleckler PJ, Jones P, et al. (2008) Consistency of modelled and observed temperature trends
677 in the tropical troposphere. Int J Climatol 28(13):1703–1722

678 Sathyendranath S, Brewin RJ, Brockmann C, Brotas V, Calton B, Chuprin A, Cipollini P,
679 Couto AB, Dingle J, Doerffer R, et al. (2019) An Ocean-Colour Time Series for Use in
680 Climate Studies: The Experience of the Ocean-Colour Climate Change Initiative (OC-CCI).
681 Sensors 19(19):4285

682 Shapiro I, Colony R, Vinje T (2003) April sea ice extent in the Barents Sea, 1850–2001. Polar
683 Res 22(1):5–10

684 Silva E, Counillon F, Brajard J, Korosov A, Pettersson LH, Samuelsen A, Keenlyside N (2021)
685 Twenty-one years of phytoplankton bloom phenology in the Barents, Norwegian, and North
686 Seas. Front Mar Sci 8:746327

687 Simmonds I, Keay K (2009) Extraordinary September Arctic sea ice reductions and their
688 relationships with storm behavior over 1979–2008. Geophys Res Lett 36(19)

689 Siswanto E (2020) Temporal variability of satellite-retrieved chlorophyll-a data in Arctic and
690 subarctic ocean regions within the past two decades. Int J Remote Sens 41(19):7427–7445

691 Smedsrud LH, Esau I, Ingvaldsen RB, Eldevik T, Haugan PM, Li C, Lien VS, Olsen A, Omar
692 AM, Otterå OH, et al. (2013) The role of the Barents Sea in the Arctic climate system. Rev
693 Geophys 51(3):415–449

694 Søreide JE, Leu EV, Berge J, Graeve M, Falk-Petersen S (2010) Timing of blooms, algal food
695 quality and *Calanus glacialis* reproduction and growth in a changing Arctic. Glob Change
696 Biol 16(11):3154–3163

697 Strass VH, Nöthig EM (1996) Seasonal shifts in ice edge phytoplankton blooms in the Barents
698 Sea related to the water column stability. Polar Biol 16(6):409–422

699 Tremblay JÉ, Bélanger S, Barber D, Asplin M, Martin J, Darnis G, Fortier L, Gratton Y,
700 Link H, Archambault P, et al. (2011) Climate forcing multiplies biological productivity in
701 the coastal Arctic Ocean. Geophys Res Lett 38(18)

702 Tuerena RE, Hopkins J, Ganeshram RS, Norman L, de la Vega C, Jeffreys R, Mahaffey C (2021)
703 Nitrate assimilation and regeneration in the Barents Sea: insights from nitrate isotopes.
704 Biogeosciences 18(2):637–653

705 Våge K, Pickart RS, Pavlov V, Lin P, Torres DJ, Ingvaldsen R, Sundfjord A, Proshutinsky A
706 (2016) The Atlantic Water Boundary Current in the Nansen Basin: Transport and mecha-
707 nisms of lateral exchange. J Geophys Res, C, Oceans 121(9):6946–6960

708 Volent Z, Johnsen G, Hovland EK, Folkestad A, Olsen LM, Tangen K, Sorensen K (2011)
709 Improved monitoring of phytoplankton bloom dynamics in a Norwegian fjord by integrating
710 satellite data, pigment analysis, and ferrybox data with a coastal observation network. J
711 Appl Remote Sens 5(1):053561

Waga H, Hirawake T (2020) Changing occurrences of fall blooms associated with variations in phytoplankton size structure in the Pacific Arctic. Front Mar Sci 7:209

Wassmann P, Ratkova T, Andreassen I, Vernet M, Pedersen G, Rey F (1999) Spring bloom development in the marginal ice zone and the central Barents Sea. Mar Ecol 20(3-4):321–346

Wassmann P, Reigstad M, Haug T, Rudels B, Carroll ML, Hop H, Gabrielsen GW, Falk-Petersen S, Denisenko SG, Arashkevich E, et al. (2006a) Food webs and carbon flux in the Barents Sea. Prog Oceanogr 71(2-4):232–287

Wassmann P, Slagstad D, Riser CW, Reigstad M (2006b) Modelling the ecosystem dynamics of the Barents Sea including the marginal ice zone: II. carbon flux and interannual variability. J Mar Syst 59(1-2):1–24

Xie J, Bertino L, Counillon F, Lisæter KA, Sakov P (2017) Quality assessment of the TOPAZ4 reanalysis in the Arctic over the period 1991-2013. Ocean Sci 13(1)

7 TABLES

Table 1: Summary table of potential mechanistic controls on autumn bloom intensity in the Barents Sea (and other regions where pertinent) and supporting or opposing evidence. Polar Front: the region of strong geographic gradients in temperature and salinity between the Atlantic and Arctic water masses.

Mechanism	Expected evidence	Supporting	Opposing	Regional expression
Wind induced mixing	Increased [*chl-a*] associated with more frequent storms	(Kogeler & Rey 1999) (Qu et al. 2020)	(Ardyna et al. 2014) (Crawford et al. 2020)	Wind induced mixing associated with autumn blooms on interior Eurasian shelves, but correlative association is weaker in the Barents Sea (Ardyna et al. 2014).
Water-column destabilised by Atlantic input	Greater Atlantic inflow into frontal regions stimulates increased [*chl-a*]; higher winds might also interact with weaker water-column stratification	(Kogeler & Rey 1999) (Oziel et al. 2017)		Nutrient rich Atlantic inflow shoals over Barents Sea Water along the southern expression of the Polar Front (Oziel et al. 2017). Continuous mixing may permit blooms to continue through summer and autumn where the Polar Front intersects the Spitsbergen bank (Kogeler & Rey 1999).
Nutrient inventory replenished by Atlantic input	Variation in Atlantic input causes variation in [*chl-a*], especially close to the inflow region	(Oziel et al. 2017) and suggested by (Hegseth 1997, Kogeler & Rey 1999)	(Oziel et al. 2017) suggests declining Atlantic nutrient inventories may undermine this mechanism	The Atlantic influenced region southwest of the southern expression of the Polar Front supports the highest September [*chl-a*] (Oziel et al. 2017). Atlantic influenced waters south of the Polar Front are sometimes observed to support autumn [*chl-a*] $>1\,\mathrm{mg\,m^{-3}}$ (Kogeler & Rey 1999).
Mixing over rough bathymetry	Modulated environmental dependencies over shallow banks	(Kogeler & Rey 1999) (Not et al. 2005)		Suggested to support continuous primary production over the Spitsbergen bank, especially where the physical structure of the Polar Front and intense tides facilitate vertical mixing (Kogeler & Rey 1999, Not et al. 2005).

Table 2: Summary of Generalised Least Squares model results. Top: independent variables. Left: dependent variables.

	B	SST	C_i	W
B		AICc = 50.58 p = 0.0028*	AICc = 45.79 p = 0.0002*	$\text{AICc}^{\text{n}}_{\text{A}}$ = 56.19 p = 0.032*
SST			AICc = 56.39 p =0.068	AICc^{n} = 56.05 p = 0.056
C_i		AICc = 56.39 p = 0.068		$\text{AICc}^{\text{n}}_{\text{A}}$ = 58.28 p = 0.30
W		$\text{AICc}^{\text{n}}_{\text{A}}$ = 55.56 p = 0.017*	AICc^{n} = 59.14 p = 0.42	

Note. GLS regressions fitted with the gls function, relating [*chl-a*] (B), SST, inflow current speed (C_i) and the windy events index (W). An 'A' subscript indicates a lag-1 autocorrelated model is preferred at an alpha level of 0.05. 'n' superscripts indicate negative relationships, while '*' denotes significance at a 0.05 alpha level. Model fits are described by their corrected Akaike Information Criterion (AICc) and p-values.

Table 3: Summary table of the results of this study.

Mechanism	Expected evidence	Supporting	Opposing	Summary
Wind induced mixing	Increased [*chl-a*] associated with more frequent storms	Supported in the far northeast	Generally not supported	Support is low
Water-column destabilised by Atlantic input	Greater Atlantic inflow into frontal regions stimulates increased [*chl-a*]	Greater Atlantic input and SST associated with higher [*chl-a*]	Greatest [*chl-a*] increases are in the inflow region, and not typically associated with fronts	Support is equivocal
Nutrient inventory replenished by Atlantic input	Variation in Atlantic input causes variation in [*chl-a*], especially close to the inflow region	Robust relationship between Atlantic inflow and [*chl-a*], especially in inflow region	Potential multi-annual feedbacks	Support is strong
Mixing over rough bathymetry	Modulated environmental dependencies over shallow banks	Bathymetry guides Atlantic inflow	Shallow banks not associated with stronger relationships	No substantial role

8 FIGURES

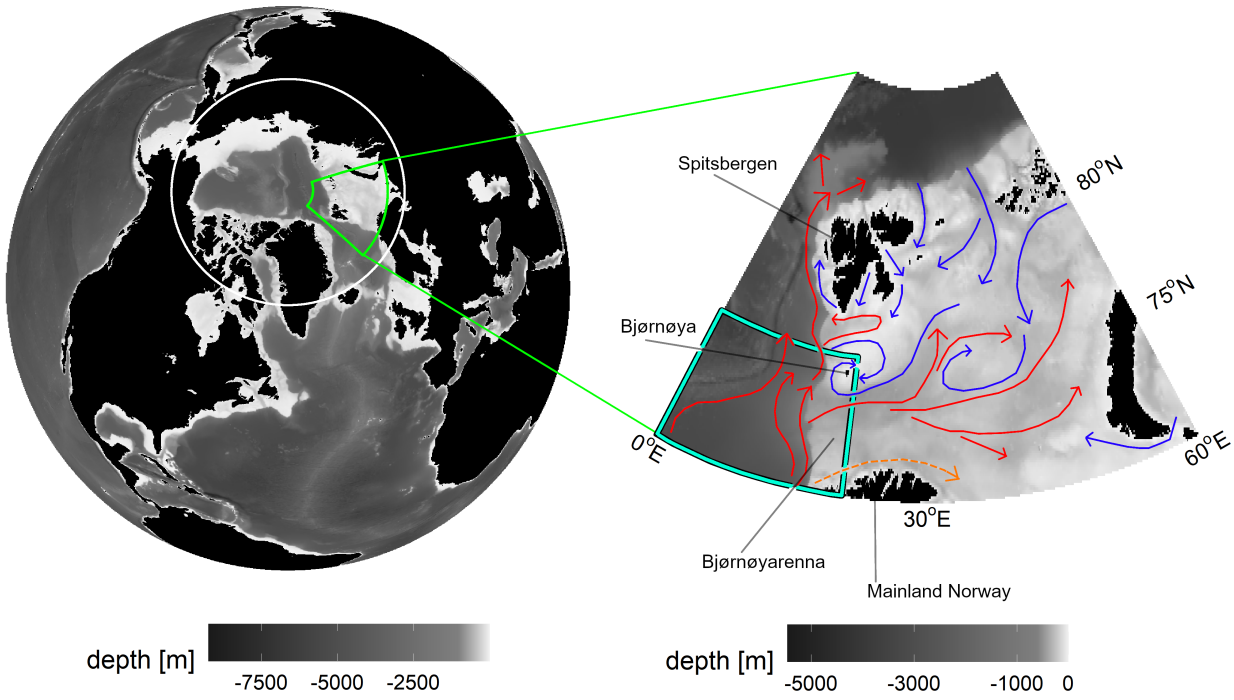

Figure 1: Left: Map of the geographic context of the Barents Sea (enclosed in green) in the Global hydrography and Arctic region (encircled in white). Right: The pattern of recirculating pathways of Atlantic (red), Arctic (blue) and Coastal (dashed orange) Water delivery, guided by its shelf topography. The primary region of Atlantic inflow is surrounded by a cyan box, (near Bjørnøyarenna). Bathymetric data were downloaded and plotted using the R marmap package (Pante & Simon-Bouhet 2013).

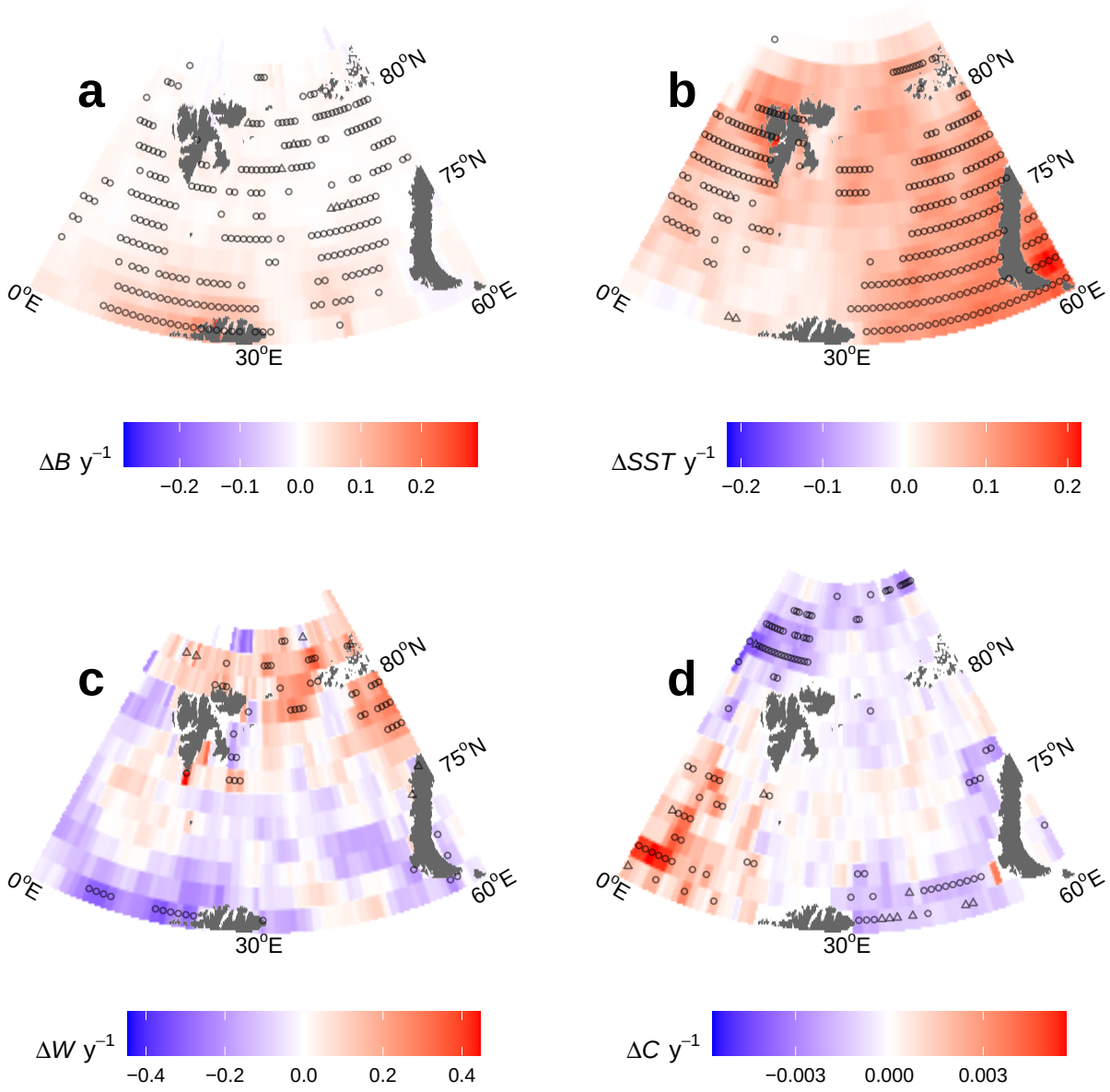

Figure 2: **Linear trends:** Slopes of linear models of the temporal evolution of [*chl-a*] (B) ($\mathrm{mg\,m^{-3}}$), Sea Surface Temperature (SST) (Kelvin), windy days (W) and current speed (C) ($\mathrm{m\,s^{-1}}$), for September between 2002 and 2019. **a)** Biomass **b)** SST **c)** Windy days **d)** Current speeds. Grid cells with significant ($p < 0.05$) trends are marked with triangles when an autocorrelated fit is preferred, and circles when a standard fit is preferred. Secular increases in biomass and SST are evident. Trends in windy days and current speeds show regional complexity. All data represent monthly integrations in September between 2002 and 2019.

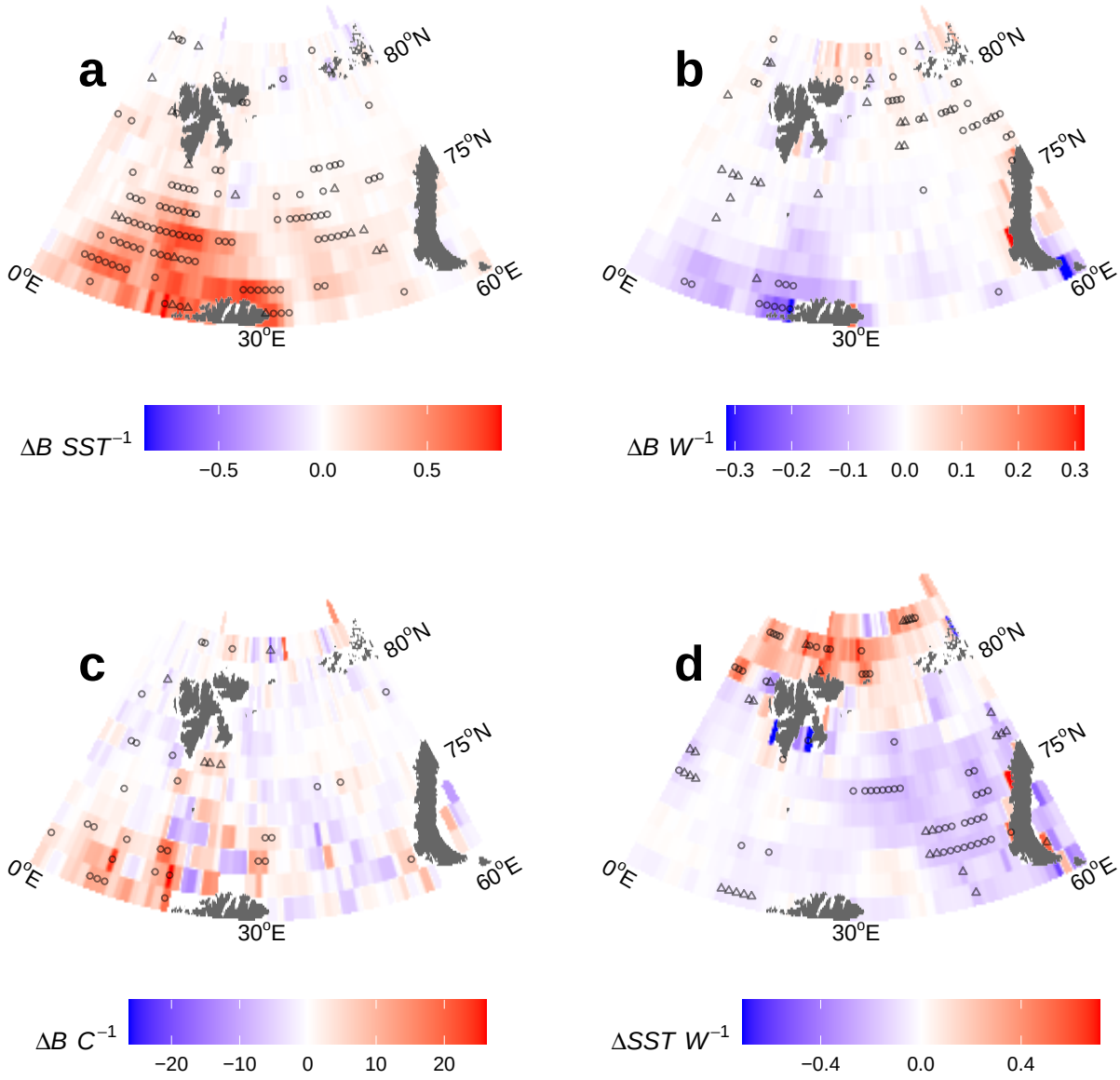

Figure 3: **Linear relationships:** Slopes of linear relationships. $[chl\text{-}a]$ (B) $(\mathrm{mg\,m^{-3}})$, SST (Kelvin), windy days (W) and current speed (C) $(\mathrm{m\,s^{-1}})$ are considered. **(a)** Biomass dependency on SST. **(b)** Biomass dependency on wind. **(c)** Biomass dependency on local currents. **(d)** SST dependency on wind. Grid cells with significant ($p < 0.05$) trends are marked with triangles when an autocorrelated fit is preferred, and circles when a standard fit is preferred. There is a strong positive relationship between biomass and SST, but not between biomass and wind. There is an ambiguous relationship of biomass and regional current speeds, and relationships between SST and winds vary between Atlantic and Arctic water masses. All data represent monthly integrations in September between 2002 and 2019.

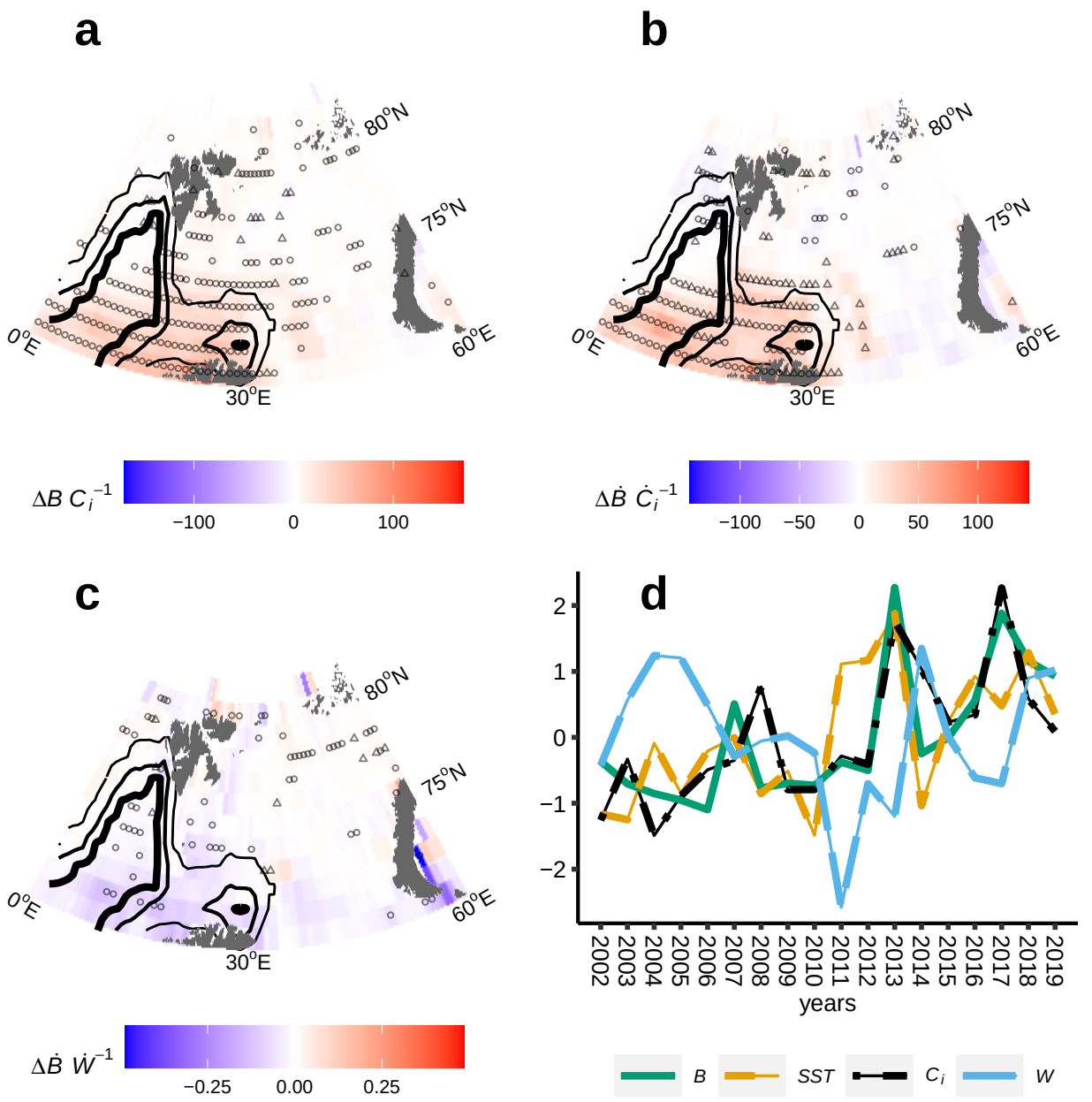

Figure 4: **Role of Atlantic inflow:** $[chl\text{-}a]$ (B) $(\mathrm{mg\,m^{-3}})$, inflow current speed (C_i) $(\mathrm{m\,s^{-1}})$, inter-annual differences of $[chl\text{-}a]$ $(\dot{B})$ $(\mathrm{mg\,m^{-3}\,yr^{-1}})$, inflow current speed $(\dot{C}_i)$ $(\mathrm{m\,s^{-1}\,yr^{-1}})$, and windy days $(\dot{W})$, are considered. **(a)** Biomass dependency on Atlantic inflow. **(b)** inter-annual differences. **(c)** Inter-annual differences of biomass and wind. **(d)** Regional variance normalised $[chl\text{-}a]$, SST, inflow current speed and windy days are presented. Grid cells with significant ($p < 0.05$) trends are marked with triangles when an autocorrelated fit is preferred, and circles when a standard fit is preferred. Thin, medium and bold contours map the 5%, 50% and 95% occurrence intervals of the geographic distribution of Atlantic Water in the time-series, based on salinity (>34.8 ‰) and temperature (>3°C). Strong positive relationships between biomass and Atlantic inflow currents are evident, especially within the region occupied by Atlantic Waters. Inter-annual variability in windiness anti-correlates with biomass. All data represent monthly integrations in September between 2002 and 2019.